In vitro apatite formation and visible-light photocatalytic activity of Ti metal subjected to chemical and thermal treatments

In vitro apatite formation and visible-light photocatalytic activity of Ti metal subjected to chemical and thermal treatments

Masakazu Kawashita[a,*], Yuto Yokohama[a], Xinyu Cui[a,b], Toshiki Miyazaki[c], Hiroyasu Kanetaka[d]

[a]*Graduate School of Biomedical Engineering, Tohoku University, Sendai 980-8579, Japan*

[b]*Institute of Metal Research, Chinese Academy of Sciences, Shenyang 110016, China*

[c]*Graduate School of Life Science and Systems Engineering, Kyushu Institute of Technology,*
Kitakyushu 808-0196, Japan

[d]*Liaison Center for Innovative Dentistry, Graduate School of Dentistry, Tohoku University,*
Sendai 980-8575, Japan

*Corresponding author

Tel.: +81-22-795-3937; Fax: +81-22-795-4735

E-mail: m-kawa@ecei.tohoku.ac.jp (M. Kawashita)

Abstract

In this study, we investigated the surface structure, apatite formation in simulated body fluid (SBF), and visible-light photocatalytic activity of Ti metal subjected to chemical and thermal treatments. Ti metal samples treated with NaOH, a nitrogen-containing

solution (0.1 M HNO_3, 0.1–1.0 M $(H_2N)_2C=O$, or 0.1–1.0 M NH_4Cl), and heat showed apatite formation on their surfaces in SBF, whereas those treated with NaOH, 0.5 or 1.0 M HNO_3, and heat did not. In the former case, apatite formation may be attributable to the fine network structure of anatase-type TiO_2 doped with a small amount of nitrogen on the surface of the Ti metal. The Ti metal treated with the latter treatment showed higher methylene blue decomposition than the untreated sample and the one treated with the former treatment. This preliminary result suggests that Ti metal treated with NaOH, 0.1 M HNO_3, and heat can potentially show visible-light-induced antibacterial property as well as bone-bonding ability.

Keywords: titanium metal; apatite; visible-light photocatalytic activity; simulated body fluid

1. Introduction

Titanium and its alloys have been widely used as artificial implants. In recent times, however, surgical site infection (SSI) has emerged as a serious problem that urgently needs a solution. To reduce the risk of SSI, many attempts have been made to develop antibacterial metallic medical devices [1-4]. We have focused on the antibacterial activity of N-doped TiO_2 under visible light [5] and tried to form this type of TiO_2 on Ti metal by surface chemical treatment. It has been reported that an anatase-type TiO_2 layer was formed on Ti metal when Ti metal was subjected to sodium hydroxide (NaOH), hot water, and heat treatment; the treated Ti metal showed apatite formation on its surface in simulated body fluid (SBF) [6]. Furthermore, Ti metal treated in this manner bonded to living bone through this apatite layer [7]. Based on these studies, we

expect that novel Ti metal with visible-light-induced antibacterial property as well as bone-bonding ability might be obtained if N-doped TiO_2 is successfully formed on Ti metal by some surface chemical treatments.

Recently, we reported that a TiO_2 layer doped with a small amount of nitrogen (~0.16 atomic%) was formed on Ti metal by NaOH, ammonia (NH_4OH), and heat treatments and that this treated Ti metal showed apatite-forming ability in SBF as well as methylene blue (MB) decomposition by visible light irradiation [8]. We also reported that Ti metal subjected to NaOH, nitric acid (HNO_3), and heat treatments showed no apatite formation in SBF although a larger amount of nitrogen (~1.1 atomic%) was doped on the Ti surface than in the earlier case. The loss of apatite-forming ability of the Ti metal subjected to NaOH, HNO_3, and heat treatments might be attributed to the dissolution of the surface $Na_{2-x}H_xTi_3O_7$ layer by acidic 1 M HNO_3 treatment [8, 9]. Therefore, if we use a lower concentration of HNO_3 or another mild acidic or neutral nitrogen-containing solution, Ti metal with a higher amount of doped nitrogen as well as apatite-forming ability in SBF might be obtained.

In this study, we attempted to form N-doped TiO_2 on Ti metal by NaOH, various concentrations of HNO_3, and heat treatments and investigated the apatite-forming ability of the samples in SBF and visible-light photocatalytic activity by examining MB decomposition. We also used a neutral urea ($(H_2N)_2C=O$) and mild acidic ammonium chloride (NH_4Cl) solution instead of HNO_3 as the nitrogen source.

2. Experimental procedure

2.1 Sample preparation

Commercially available pure Ti plates (10 mm × 10 mm × 1 mm; purity:

99.9%; Kojundo Chemical Laboratory, Japan) were used. They were abraded using No. 400 abrasive diamond paper and then washed with pure acetone and ultrapure water in an ultrasonic cleaner. The Ti plates were soaked in 5 mL of 5 M NaOH solution at 60°C. The samples were subsequently soaked in 7 mL of either 0.1–1 M HNO_3, urea, or NH_4Cl at 40°C for 24 h and were then gently washed with ultrapure water and dried. Special grade NaOH, HNO_3, $(H_2N)_2C=O$, and NH_4Cl were used in this study. All of these chemicals were purchased from Wako Pure Chemical Industries, Japan. The samples were heated to 600°C at a rate of 5°C·min^{-1} in an electric furnace (FO-100, Yamato Scientific, Japan), maintained at this temperature for 1 h, and then naturally cooled in the furnace to room temperature. Table 1 lists the abbreviated names of the samples subjected to various treatments.

2.2 Immersion of samples in SBF

The samples were soaked in 30 mL of SBF [10, 11] containing ion concentrations (Na^+: 142.0 mM; K^+: 5.0 mM; Ca^{2+}: 2.5 mM; Mg^{2+}: 1.5 mM; Cl^-: 147.8 mM; HCO_3^-: 4.2 mM; HPO_4^{2-}: 1.0 mM; SO_4^{2-}: 0.5 mM) that were nearly identical to those in human blood plasma at 36.5°C according to the ISO 23317: 2012 standard. After the samples had been immersed in SBF for 7 days, they were removed and gently washed with ultrapure water.

2.3 Characterization of sample surfaces

The surface structures of the samples were investigated using a thin-film X-ray diffractometer (TF-XRD; RINT-2200VL, Rigaku, Japan; X-ray source: Ni-filtered Cu Kα radiation; X-ray power: 40 kV, 40 mA; scanning rate: 2° min^{-1}; sampling angle:

0.02°), scanning electron microscope (SEM; VE-8800, Keyence, Japan), and X-ray photoelectron spectrometer (XPS; AXIS Ultra DLD, Kratos Analytical, UK; X-ray source: monochromatic Al Kα radiation (1486.7 eV); X-ray power: 15 kV, 10 mA). Furthermore, in XPS, the binding energy was calibrated using the C_{1s} photoelectron peak at 284.8eV as a reference. XPS peak analysis was performed using CasaXPS Version 2.3.15 software with all spectra Shirley background subtracted prior to fitting. The elemental composition was calculated from XPS spectra using the specific relative sensitivity factors for the Kratos Axis Ultra (O_{1s}: 0.78, Ti_{2p}: 2.001, N_{1s}: 0.477, C_{1s}: 0.278).

2.4 Evaluation of visible-light photocatalytic activity

The visible-light photocatalytic activity of the samples was evaluated by examining MB decomposition (Waldeck, Germany). The samples were soaked in 5 mL of 0.01 mM MB aqueous solution and incubated for 24 h to reach adsorption equilibrium. The MB aqueous solution was then replenished, and the samples were irradiated using two fluorescent lights (FL20SSEX-N/18X, NEC, Japan and FL20SS·N/18, Panasonic, Japan) for 6 h through an ultraviolet cutting filter (HGS05S, Lintec Commerce, Japan). The resultant cut-off wavelength was 350 nm and the distance between the sample and the filter was ~6 cm. The incident radiant flux density was fixed at 30 W/m^2. The MB concentration in the irradiated samples was examined using an ultraviolet visible (UV-VIS) spectrophotometer (PD-303, Apel, Japan) by measuring the UV absorbance at 664 nm. The MB concentration was also measured in unsoaked samples as a control. Three samples for each treatment condition were subjected to the above evaluation. The decrease in MB concentration (%) was calculated based on the difference in the MB

concentration in the soaked and unsoaked samples, C_{sample} and C_{blank}, respectively, as follows [12]:

$$\text{Decrease in concentration (\%)} = (C_{blank} - C_{sample}) \times 100/C_{blank} \quad (1)$$

3. Results and discussion

3.1 Surface structure of samples

Figure 1 shows SEM photographs of the samples subjected to different treatments. A fine network structure that was typically formed on the sample after NaOH and heat treatments [13] was partially observed for the sample treated in 0.1 M HNO_3, whereas the samples treated in 0.5 and 1.0 M HNO_3 showed flat surfaces as did the untreated sample. In samples treated in $(NH_2)_2C=O$ and NH_4Cl, the fine network structure almost remained irrespective of the concentrations.

Figure 2 shows TF-XRD patterns of the samples subjected to different treatments. Samples treated in 0.5 or 1.0 M HNO_3 showed diffraction peaks ascribed to rutile-type TiO_2 (PDF #21-1276) and α-Ti (PDF #44-1294). Furthermore, they showed diffraction peaks ascribed to only α-Ti before heat treatment (data not shown), suggesting that the surface layer formed by NaOH treatment was completely dissolved by 0.5 or 1.0 M HNO_3 treatment. The dissolution of the surface layer is assumable from the flat surface of these samples, as shown in Fig. 1. Therefore, rutile-type TiO_2 is formed by simple

thermal oxidation of the Ti metal. The sample treated in 0.1 M HNO_3 showed small diffraction peaks ascribed to anatase-type TiO_2 (PDF #21-1272) in addition to those ascribed to rutile-type TiO_2 and α-Ti. The samples treated in $(NH_2)_2C=O$ and NH_4Cl showed diffraction peaks of anatase-type TiO_2, rutile-type TiO_2, and α-Ti. The samples that formed anatase-type TiO_2 had hydrogen titanate ($H_2Ti_3O_7$) or sodium hydrogen titanate ($Na_{2-x}H_xTi_3O_7$) on their surfaces before heat treatment (data not shown), suggesting that $H_2Ti_3O_7$ or $Na_{2-x}H_xTi_3O_7$ is transformed into anatase-type TiO_2 by the heat treatment, as reported in previous studies [8, 9]. Here, it should be noted that the intensity of the diffraction peak of anatase-type TiO_2 was larger than that of rutile-type TiO_2 for samples treated in $(NH_2)_2C=O$ and NH_4Cl, suggesting that anatase-type TiO_2 was mainly precipitated on the samples treated in $(NH_2)_2C=O$ and NH_4Cl.

Figure 3 shows Na_{KLL} and N_{1s} XPS spectra of the samples. All samples showed an Na_{KLL} peak, ascribed to Na-O [13], at ~497 eV and an N_{1s} peak at ~400 eV. The samples treated in HNO_3 showed an additional N_{1s} peak at ~402 eV. The intensity of this peak increased with the HNO_3 concentration. The N_{1s} peaks at ~400 and ~402 eV are ascribed to N-O and N-O-Ti, respectively [14, 15]. These results suggest that the chemical state of N in the samples treated in HNO_3 differs from that in other samples. Furthermore, all samples showed Ti_{2p} peaks at ~458.5 and ~464 eV and O_{1s} peaks at

~530 eV. These peaks are ascribed to Ti-O in TiO_2 (data not shown) [16, 17, 18].

Table 1 shows the Na and N contents of samples as calculated from the areas of the XPS peaks. The Na contents for samples treated in $(NH_2)_2C=O$ were higher than those for other samples, and they decreased with increasing $(NH_2)_2C=O$ concentration. The higher Na content for samples in $(NH_2)_2C=O$ is attributed to the neutrality of the $(NH_2)_2C=O$ solution. When NaOH-treated Ti metal is treated in HNO_3 or NH_4Cl solution, the surface layer of $Na_{2-x}H_xTi_3O_7$ might be dissolved [8, 9] and/or Na might be rapidly released from $Na_{2-x}H_xTi_3O_7$ because the HNO_3 and NH_4Cl solutions are acidic and mildly acidic, respectively. In contrast, when NaOH-treated Ti metal is treated in $(NH_2)_2C=O$ solution, the surface layer of $Na_{2-x}H_xTi_3O_7$ might not be dissolved and Na release might not be remarkable, resulting in the higher Na content, although the Na release increased slightly with the $(NH_2)_2C=O$ concentration.

The N contents for samples treated in HNO_3 were higher than those for other samples and they increased with the HNO_3 concentration, suggesting that HNO_3 treatment is more effective for nitrogen doping than $(NH_2)_2C=O$ or NH_4Cl treatment. The nitrogen doping efficiency is related to the state of nitrogen in the treatment solutions. When Ti metal is treated in NaOH solution, hydrated TiO_2 and $HTiO_3^-$ are formed on the Ti metal surface as follows [13].

$$TiO_2 \cdot nH_2O + OH^- \leftrightarrow HTiO_3^- \cdot nH_2O \quad (1)$$

$HTiO_3^-$ might be substituted with NO_3^- by HNO_3 treatment because NO_3^- is slightly smaller than $HTiO_3^-$ [19, 20]. However, $(NH_2)_2C=O$ is non-electrolytic, and therefore, it might not easily incorporate into the NaOH-treated Ti metal surface. In NH_4Cl solution, nitrogen exists in the form of NH_4^+. NH_4^+ is likely to be incorporated into the sample surface via ion exchange with Na^+ and/or H_3O^+; however, such incorporation hardly occurred because the ionic radius of NH_4^+ (151 pm) is larger than that of Na^+ (116 pm) [21].

3.2 Apatite-forming ability of samples

Figure 4 shows SEM photographs of the samples after soaking in SBF. After SBF soaking, no change in surface morphology was observed for the samples treated in 0.5 or 1.0 M HNO_3; however, some deposits were formed for samples treated in 0.1 M HNO_3. Similar deposits were also observed for samples treated in $(NH_2)_2C=O$ or NH_4Cl solution irrespective of the solution concentration. It should be noted that a dense and uniform layer was deposited on the samples treated in $(NH_2)_2C=O$ solution.

Figure 5 shows the TF-XRD patterns of samples after soaking in SBF. Diffraction

peaks ascribed to apatite were newly observed for samples treated in 0.1 M HNO_3 and $(NH_2)_2C=O$ or NH_4Cl solution, whereas they were not observed for samples treated in 0.5 or 1.0 M HNO_3. Therefore, it is believed that the deposits observed on some samples after soaking in SBF (see Fig. 4) are apatite.

According to the TF-XRD patterns of samples before soaking in SBF (Fig. 2), all the samples that formed apatite in SBF precipitated anatase-type TiO_2. Therefore, we can speculate that anatase-type TiO_2 plays an important role in apatite deposition in SBF [6, 8, 22].

Figure 4 shows that the apatite-forming ability of the samples treated in $(NH_2)_2C=O$ solution was better than that of samples treated in other solutions. This can be interpreted from the higher Na content (see Table 1) on the surfaces of samples treated in $(NH_2)_2C=O$ solution. When Ti metal subjected to NaOH and heat treatments is soaked in SBF, Na^+ ions are released via ion exchange with H_3O^+ to increase the pH of the surrounding SBF, resulting in the enhancement of apatite formation; simultaneously, the release of Na^+ ions leads to the formation of Ti-OH groups that are effective for apatite nucleation [23, 24].

3.3 Visible light photocatalytic activity of samples

Figure 6 shows the decrease in the MB concentration in samples immersed in MB

solution and irradiated with visible light. Untreated Ti showed a low decomposition rate of ~1%. Samples treated in HNO_3 and $(NH_2)_2C=O$ showed MB decomposition rates of ~8% and ~4%, respectively; however, those treated in NH_4Cl solution showed a low MB decomposition rate similar to that of the untreated sample. The higher MB deposition rate of samples treated in HNO_3 than those of samples treated in other solutions can be attributed to the higher amount of nitrogen doping (see Table 1). Furthermore, there is no remarkable difference between MB decomposition in samples treated in HNO_3 with different concentrations. According to these results and those shown in Table 1, the N content and crystalline phase of TiO_2 have little effect on the MB decomposition ability of the samples, although the mechanism of the same remains unclear.

Unexpectedly, the samples treated in $(NH_2)_2C=O$ showed a slightly higher decomposition rate than those treated in NH_4Cl, although the N content on the sample surfaces (see Table 1) and crystalline phase of TiO_2 (see Fig. 2) was almost the same between these two samples. To interpret this result, we have to consider a reaction other than the photocatalytic reaction. Here, it should again be noted that a larger amount of Na remained in samples treated in $(NH_2)_2C=O$ than in the samples treated in NH_4Cl (see Table 1). Therefore, when the samples treated in $(NH_2)_2C=O$ are soaked in MB solution,

the pH of the MB solution might increase locally at the sample surface via ion exchange of Na^+ with H_3O^+, resulting in a basic condition on the sample surface. Under the basic condition, MB will change into leucomethylene blue and/or azure B [25], which might be observed as a decrease in the MB concentration. Leucomethylene blue show no absorption at ~664 nm in the absorption wavelength of MB, and azure B shows an absorption peak at ~645 nm [25]. This means that if azure B is mainly formed, the color of the MB solution will change somewhat. However, in this study, the MB solution did not show a remarkable change in color. We did not confirm the absorption peak shift of the MB solution owing to the soaking of the samples by the spectrometer; however, the present results suggest that leucomethylene blue might be mainly formed by the soaking of the samples treated in $(NH_2)_2C=O$.

No study has yet conclusively reported on the relationship between MB decomposition ability and antibacterial activity, and therefore, it is essential to evaluate the antibacterial activity of the present samples in future work. However, we speculate that the MB decomposition rate of the present samples (~8%) is still low and not enough to show sufficient antibacterial activity. A much higher MB decomposition rate is believed to be achieved if the amount and chemical state of doped nitrogen is precisely controlled, because nitrogen-doped TiO_2 prepared by electron beam deposition

actually showed a high decrease in the MB concentration of ~40% by visible light irradiation for 6 h with an incident radiant flux density of 15.1 W/m^2 [26]. Further studies are currently underway to determine the surface treatment condition for improving the MB decomposition ability of samples.

4. Conclusions

We investigated the surface structure, apatite formation in SBF, and visible-light photocatalytic activity of Ti metal subjected to chemical and thermal treatments. When Ti metal is subjected to NaOH, 0.1 M HNO_3, and heat treatments, anatase-type TiO_2 doped with a small amount of nitrogen was formed on the Ti metal. Therefore, the treated Ti metal showed apatite formation on its surface in SBF and MB decomposition upon visible light irradiation. When we use $(NH_2)_2C=O$ and NH_4Cl instead of HNO_3, anatase-type TiO_2 doped with a small amount of nitrogen was again formed on the Ti metal and apatite formation in SBF was confirmed irrespective of the solution concentrations; however, the MB decomposition rate of these samples was lower than that of the samples treated in HNO_3.

Acknowledgements

The authors would like to thank Ms. Omura and Prof. Goto of the Institute for Materials Research, Tohoku University, for their assistance with the XPS measurement and data analysis. This work was partially supported by JSPS KAKENHI Grant Numbers 2465027 and 25282139.

References

[1] W. Chen, Y. Liu, H.S. Courtney, M. Bettenga, C.M. Agrawal, J.D. Bumgardner, J.L. Ong, In vitro anti-bacterial and biological properties of magnetron co-sputtered silver-containing hydroxyapatite coating, Biomaterials 27 (2006) 5512–5517.

[2] I. Noda, F. Miyaji, Y. Ando, H. Miyamoto, T. Shimazaki, Y. Yonekura, M. Miyazaki, M. Mawatari, T. Hotokebuchi, Development of novel thermal sprayed antibacterial coating and evaluation of release properties of silver ions, J. Biomed. Mater. Res. Part B: Appl. Biomater. 89B (2009) 456–465.

[3] T. Shirai, T. Shimizu, K. Ohtani, Y. Zen, M. Takaya, H. Tsuchiya, Antibacterial iodine-supported titanium implants, Acta Biomater. 7 (2011) 1928–1933.

[4] H. Tsuchiya, T. Shirai, H. Nishida, H. Murakami, T. Kabata, N. Yamamoto, K. Watanabe, J. Nakase, Innovative antimicrobial coating of titanium implants with iodine, J. Orthop. Sci. 17 (2012) 595–604.

[5] M.-S. Wong, W.-C. Chu, D.-S. Sun, H.-S. Huang, J.-H. Chen, P.-J. Tsai, N.-T. Lin, M.-S. Yu, S.-F. Hsu, S.-L. Wang, H.-H. Chang, Visible-light-induced bactericidal activity of a nitrogen-doped titanium photocatalyst against human pathogens, Appl. Environ. Microbiol. 72 (2006) 6111–6116.

[6] M. Uchida, H.-M. Kim, T. Kokubo, S. Fujibayashi, T. Nakamura, Effect of water treatment on the apatite-forming ability of NaOH-treated titanium metal, J. Biomed.

Mater. Res. 63 (2002) 522–530.

[7] S. Fujibayashi, T. Nakamura, S. Nishiguchi, J. Tamura, M. Uchida, H.-M. Kim, T. Kokubo, Bioactive titanium: effect of sodium removal on the bone-bonding ability of bioactive titanium prepared by alkali and heat treatment, J. Biomed. Mater. Res. 56 (2001) 562–570.

[8] M. Kawashita, N. Matsui, T. Miyazaki, H. Kanetaka, Effect of ammonia or nitric acid treatment on surface structure, in vitro apatite formation, and visible-light photocatalytic activity of bioactive titanium metal, Colloids Surf., B 111 (2013) 503–508.

[9] D. Pattanayak, S. Yamaguchi, T. Matsushita, T. Kokubo, Nanostructured positively charged bioactive TiO_2 layer formed on Ti metal by NaOH, acid and heat treatment, J. Mater. Sci.: Mater. Med. 22 (2011) 1803–1812.

[10] S.B. Cho, K. Nakanishi, T. Kokubo, N. Soga, C. Ohtsuki, T. Nakamura, T. Kitsugi, T. Yamamuro, Dependence of apatite formation on silica gel on its structure: Effect of heat treatment, J. Am. Ceram. Soc. 78 (1995) 1769–1774.

[11] T. Kokubo, H. Takadama, How useful is SBF in predicting in vivo bone bioactivity? Biomaterials, 27 (2006) 2907–2915.

[12] M. Kamitakahara, O. Kawaguchi, N. Watanabe, K. Ioku, Characterisation and

photocatalytic activity of structure-controlled spherical granules of an anatase/hydroxyapatite composite, Mater. Res. Bull. 46 (2011) 2283–2287.

[13] H.-M. Kim, F. Miyaji, T. Kokubo, T. Nakamura, Preparation of bioactive Ti and its alloys via simple chemical surface treatment, J. Biomed. Mater. Res. 32 (1996) 409–417.

[14] A. Barrie, F. J. Street, An Auger and X-ray photoelectron spectroscopic study of sodium metal and sodium oxide, J. Electron Spectrosc. Relat. Phenom. 7 (1975) 1–31.

[15] D. Wu, L. Wan, Low-temperature synthesis of anatase C-N-TiO_2 photocatalyst with enhanced visible-light-induced photocatalytic activity, Appl. Surf. Sci. 271 (2013) 357–361.

[16] M. Hashimoto, K. Hayashi, S. Kitaoka, Enhanced apatite formation on Ti metal heated in P_{O2}-controlled nitrogen atmosphere, Mater. Sci. Engin. C 33 (2013) 4155–4159.

[17] T.K. Sham, M.S. Lazarus, X-ray photoelectron spectroscopy (XPS) studies of clean and hydrated TiO_2 (rutile) surfaces, Chem. Phys. Lett., 68 (1979) 426–432.

[18] Y. Nakano, A. Sugino, K. Tsuru, K. Uetsuki, Y. Shirosaki, S. Hayakawa, A. Osaka, Enhancement of apatite-forming ability of parallely aligned Ti-substrates with optimum gaps by autoclaving, J. Ceram. Soc. Jpn. 118 (2011) 483–486.

[19] M.M. Bursey, D.J. Harvan, L.G. Pedersen, A.T. Maynard, Direct observation of the hydrogen metatitanate ($HTiO_3^-$) ion, Inorg. Chem., 24 (1985) 4748–4749.

[20] Comprehensive Inorganic Chemistry, in: J.C. Bailar, H.J. Emeléus, R. Nyholm, A.F. Trotman-Dickenson (eds.), Pergamon Press Ltd., Oxford, 1973, p. 382.

[21] J. E. Huheey, Inorganic Chemistry: Principles of Structure and Reactivity, third ed., Harper & Row, New York, 1983, p. 74 and p. 78.

[22] M. Kawashita, N. Matsui, T. Miyazaki, H. Kanetaka, Effect of autoclave and hot water treatments on surface structure and in vitro apatite-forming ability of NaOH- and heat-treated bioactive titanium metal, Mater. Trans. 54 (2013) 811–816.

[23] T. Kokubo, H.-M. Kim, M. Kawashita, Novel bioactive materials with different mechanical properties, Biomaterials 24 (2003) 2161–2175.

[24] T. Kokubo, H.-M. Kim, M. Kawashita, T. Nakamura, Bioactive metals: preparation and properties, J. Mater. Sci.: Mater. Med. 15 (2004) 99–107.

[25] A. Mills, D. Hazafy, J. Parkinson, T. Tuttle, M.G. Hutchings, Effect of alkali on methylene blue (C.I. Basic Blue 9) and other thiazine dyes, Dyes Pigm. 88 (2011) 149–155.

[26] T.-S. Yang, M.-C. Yang, C.-B. Shiu, W.-K. Chang, M.-S. Wong, Effect of N_2 ion flux on the photocatalysis of nitrogen-doped titanium oxide films by electron-beam evaporation, Appl. Surf. Sci. 252 (2006) 3729–3736.

Figure legends

Fig. 1 SEM photographs of Ti metal subjected to various surface treatments.

Fig. 2 TF-XRD patterns of Ti metal subjected to various surface treatments.

Fig. 3 Na_{KLL} and N_{1s} XPS spectra of Ti metal subjected to various surface treatments.

Fig. 4 SEM photographs of Ti metal subjected to various surface treatments and then soaked in SBF for 7 days.

Fig. 5 TF-XRD patterns of Ti metal subjected to various surface treatments and then soaked in SBF for 7 days.

Fig. 6 Decrease in MB concentration upon visible light irradiation of immersed samples (mean ± SD, n = 3).

Table legends

Table 1 Crystalline phases and Na and N contents on surfaces of samples subjected to various surface treatments.

Figure

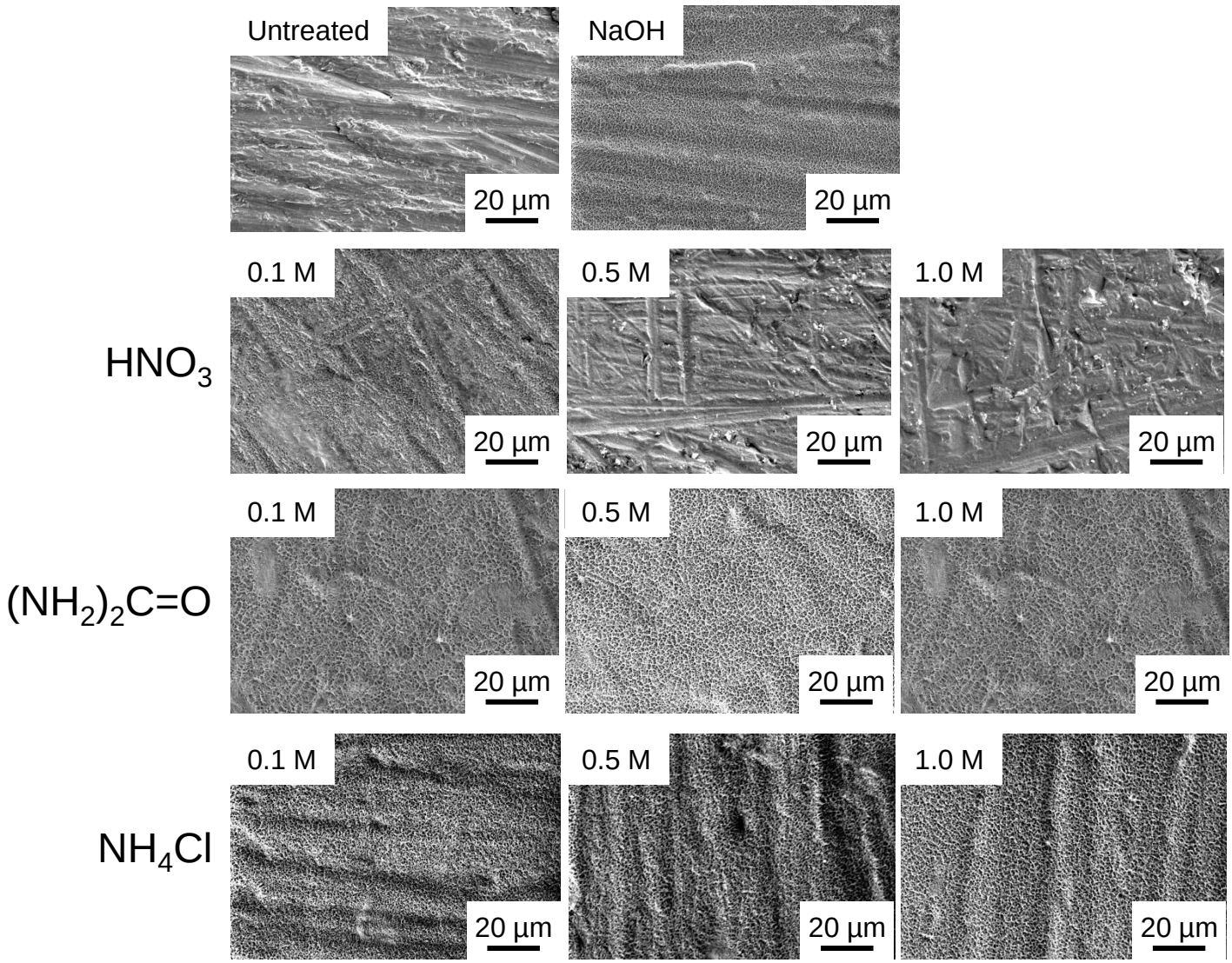

Figure 1 M. Kawashita et al.

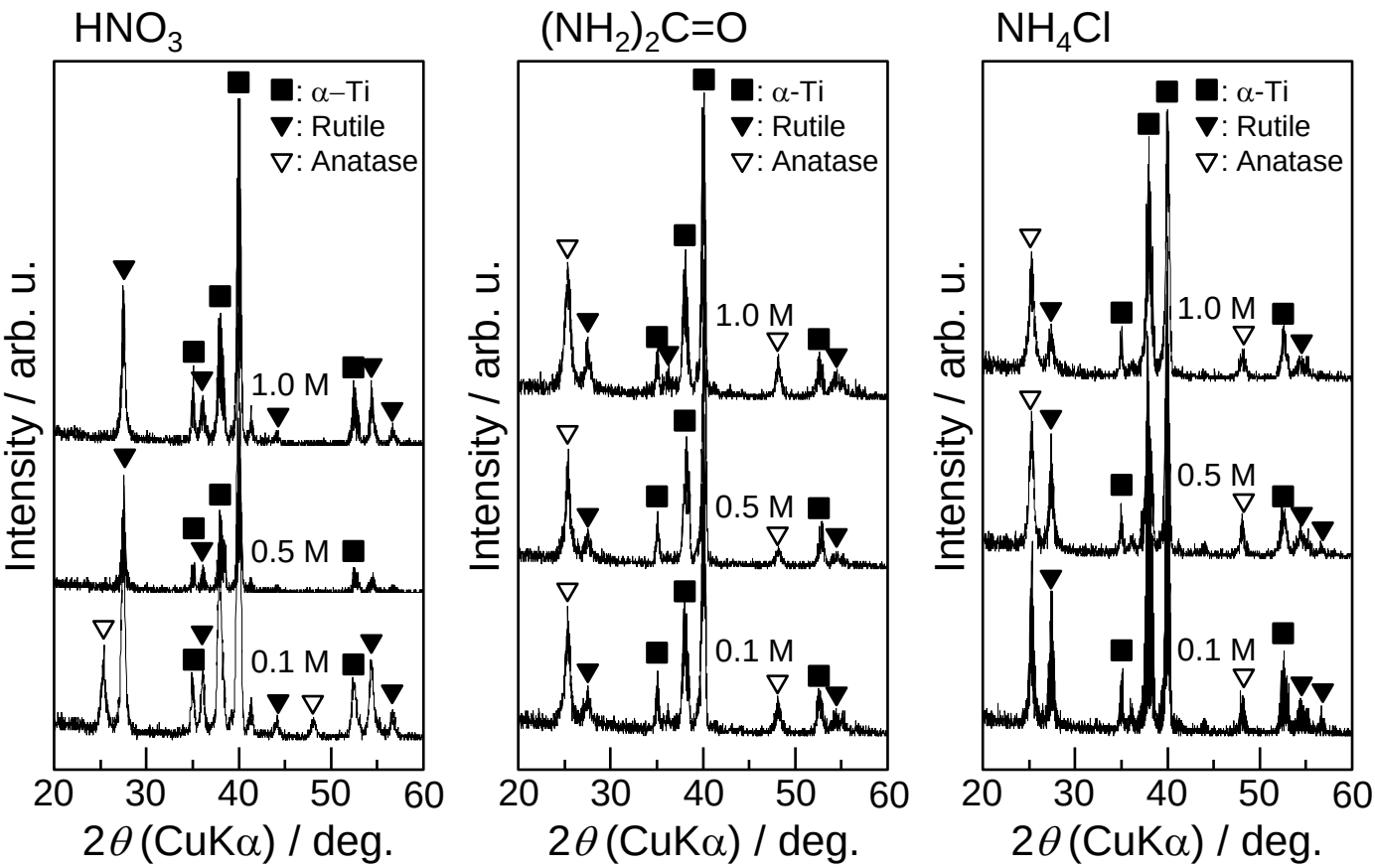

Figure 2 M. Kawashita et al.

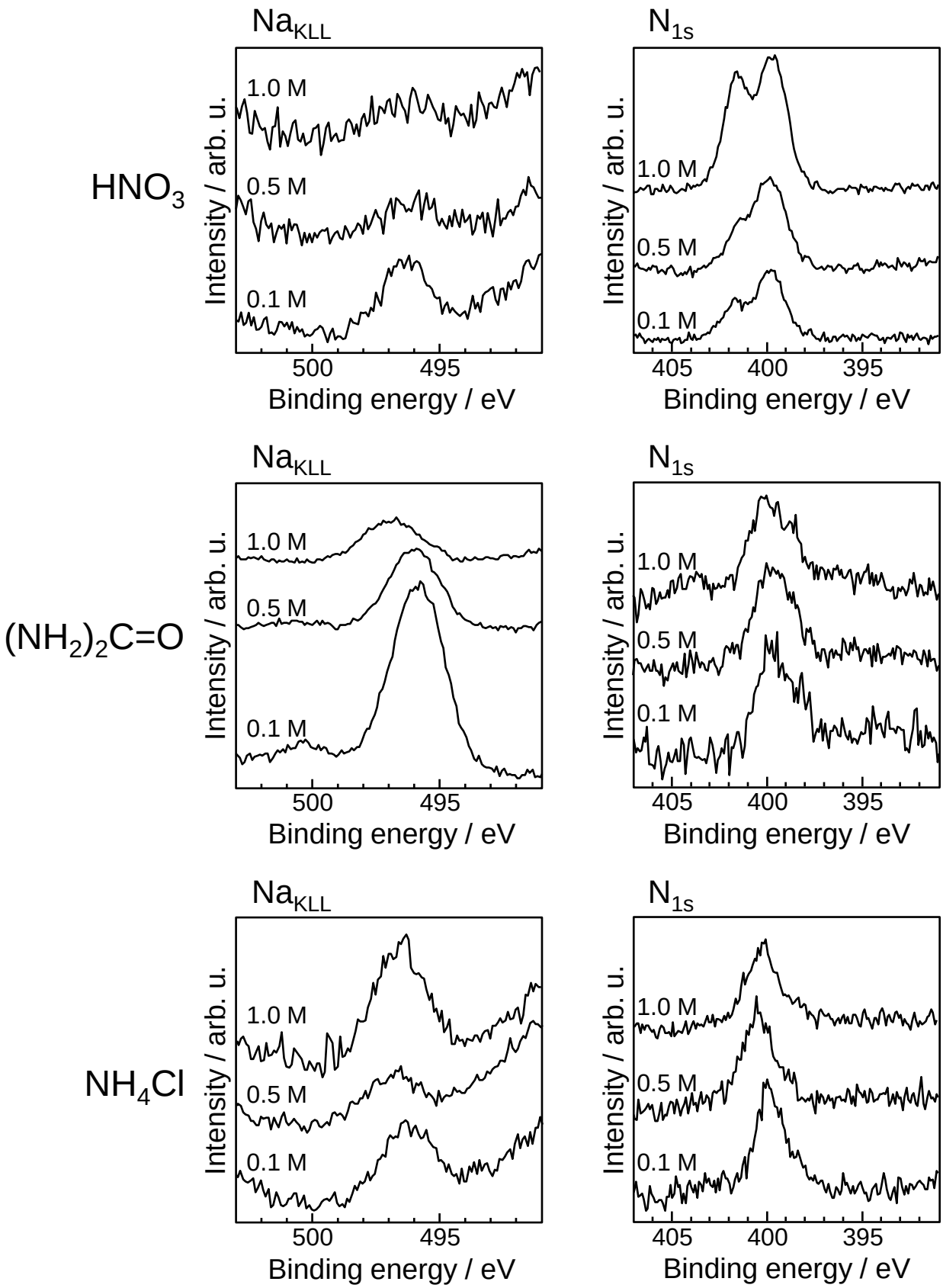

Figure 3 M. Kawashita *et al.*

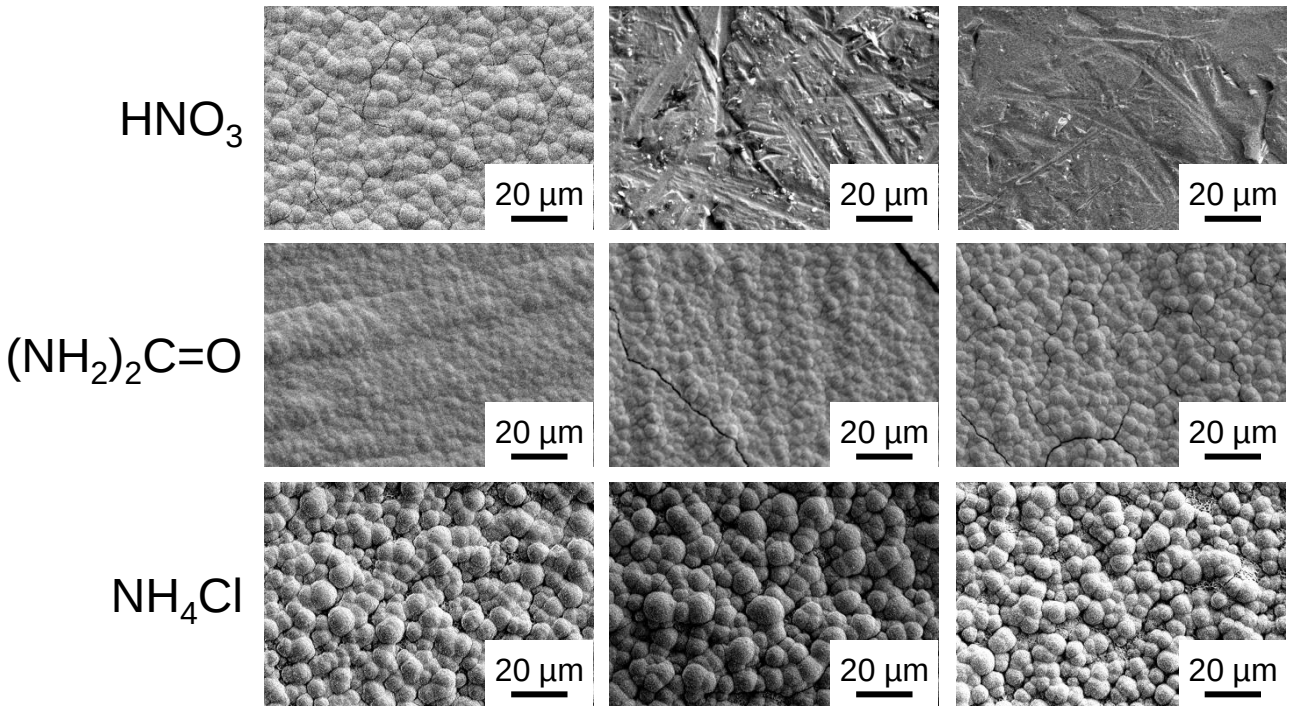

Figure 4 M. Kawashita *et al.*

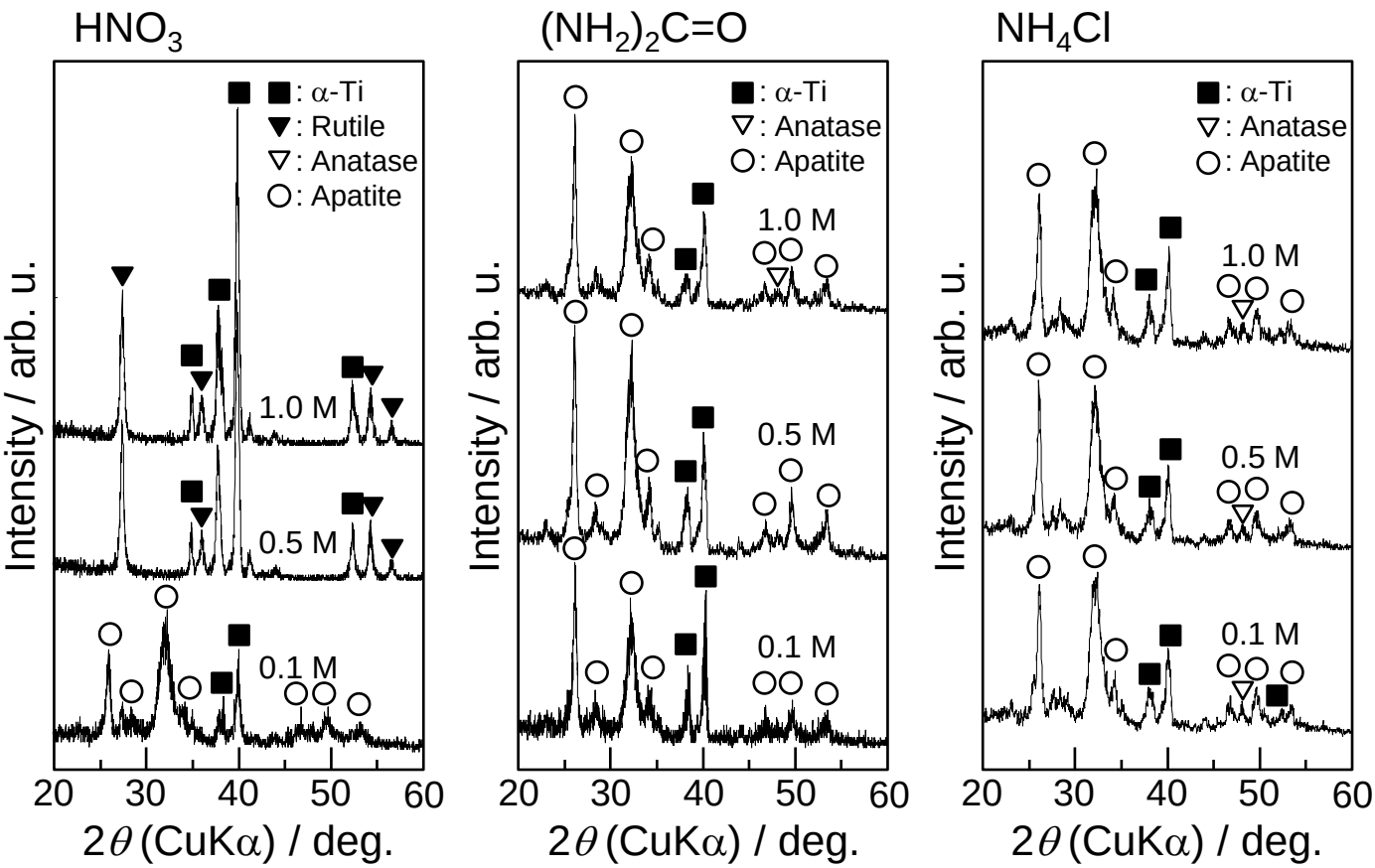

Figure 5 M. Kawashita *et al.*

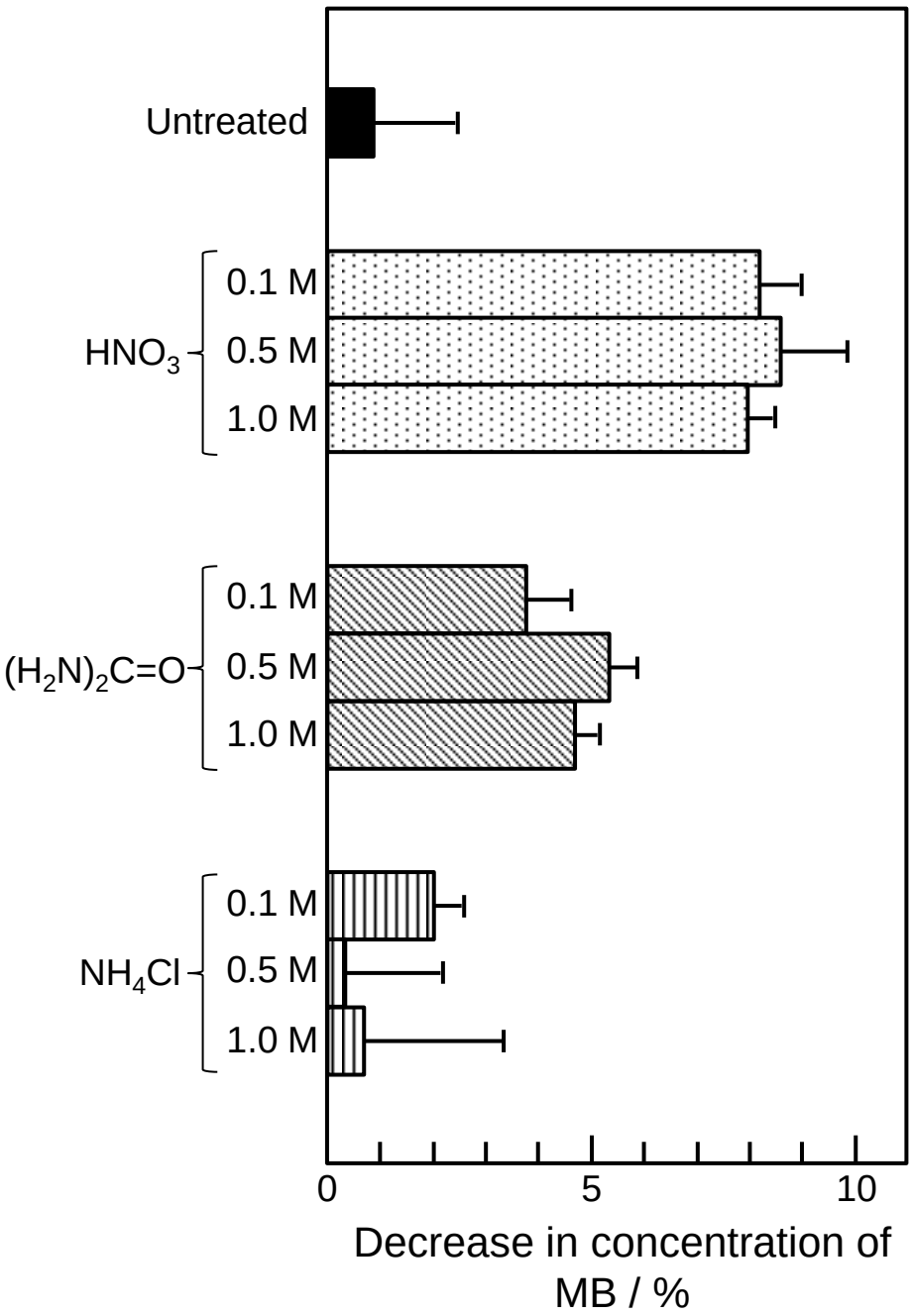

Figure 6 M. Kawashita *et al.*

Table 1
Crystalline phases and Na and N contents on surfaces of samples subjected to various surface treatments.

Reagents	Concentration of reagent (M)	Crystalline phase	Na content (atomic%)	N content (atomic%)
HNO_3	0.1	Ti, Rutile, Anatase	0.28	0.73
	0.5	Ti, Rutile	0.11	0.87
	1.0	Ti, Rutile	0.13	1.63
$(NH_2)_2C=O$	0.1	Ti, Anatase	5.7	0.22
	0.5	Ti, Anatase	2.36	0.22
	1.0	Ti, Anatase	1.21	0.21
NH_4Cl	0.1	Ti, Anatase	0.35	0.23
	0.5	Ti, Anatase	0.17	0.22
	1.0	Ti, Anatase	0.64	0.21